Virology 401 (2010) 80–89

Contents lists available at ScienceDirect

Virology

journal homepage: www.elsevier.com/locate/yviro

A flavivirus signal peptide balances the catalytic activity of two proteases and thereby facilitates virus morphogenesis

Mario Lobigs [a,*], Eva Lee [a], Mah Lee Ng [b], Megan Pavy [a], Päivi Lobigs [a]

[a] John Curtin School of Medical Research, The Australian National University, Canberra, ACT 2601, Australia
[b] Department of Microbiology, National University of Singapore, Singapore 117597

ARTICLE INFO

Article history:
Received 3 December 2009
Returned to author for revision
30 December 2009
Accepted 5 February 2010
Available online 6 March 2010

Keywords:
Flavivirus
Virus assembly
Polyprotein processing
Signal peptide

ABSTRACT

Two cleavages on either side of a signal peptide separating capsid and prM on the nascent flavivirus polyprotein are uniquely regulated, such that cytosolic capsid cleavage triggers signalase cleavage of prM. Here, we show, using two experimental approaches, that this sequential order of cleavages facilitates virus morphogenesis: (i) A Murray Valley encephalitis virus (MVEV) variant, in which both cleavages occurred efficiently and independently of each other, displayed an assembly defect. (ii) Replicon particle assembly was assayed in packaging cells encoding the MVEV structural proteins; bicistronic expression of either mature or membrane-anchored capsid in addition to that of the prM and E proteins showed enhanced particle production in the latter cell line. Taken together, this study demonstrates that efficient flavivirus assembly requires a cleavable transmembrane anchor of C protein and an obligatory order of cleavages at the C–prM junction, both controlled by sequence elements in the prM signal peptide.

Introduction

The positive-strand RNA genome of the flaviviruses is ~10.8 kb in length. It is translated into a single polyprotein, which traverses the membranes of the endoplasmic reticulum (ER) multiple times and is proteolytically cleaved into at least 10 viral proteins: 3 structural proteins (capsid [C], precursor to membrane [prM], and envelope [E]) and 7 nonstructural proteins (NS1 through to NS5). All cytoplasmic cleavages of the polyprotein are catalysed by a virally encoded protease composed of the NS3 protein and its NS2B cofactor, whereas the ER luminal cleavages are mediated by the cellular enzyme, signal peptidase (reviewed in Lindenbach and Rice, 2001). The protease, which cleaves the C-terminus of the NS1 protein, remains elusive.

Flaviviral gene expression from the polycistronic mRNA exploits diverse strategies for increasing the coding capacity of the genome and/or viral replication efficiency. We and others have described a mechanism, so far unique among the flaviviruses, which controls the sequential order of two cleavages between the C and prM proteins (Amberg et al., 1994; Amberg and Rice, 1999; Lee et al., 2000; Stocks and Lobigs, 1998; Yamshchikov and Compans, 1993). It involves the regulation of ER luminal signalase cleavage of prM by the viral NS2B-3 protease, which catalyses an upstream cleavage at the cytoplasmic side of the signal peptide to generate mature C protein (Lobigs, 1993). Thus, signalase cleavage of prM remains inefficient until the cleavage of C protein has taken place (Stocks and Lobigs, 1998). Remarkably, the signalase cleavage of prM can be induced posttranslationally by trypsin digestion of the C protein on microsomal membranes isolated from cells expressing uncleaved C–prM precursor (Stocks and Lobigs, 1995). Signal peptides have a three-region design, consisting of a (+) charged N-terminal (n-region), a hydrophobic central (h-region) and a polar C-terminal region (c-region) (von Heijne, 1990). To uncouple the sequential order of cleavages at the C–prM junction, we have introduced polar amino acids into the C-terminal region of the prM signal peptide to generate a signal sequence with an "idealised" c-region. This approach elicited efficient cleavage of prM independent of prior cleavage of C protein by the NS2B-3 protease in two mosquito-borne flavivirus models (Murray Valley encephalitis virus [MVEV] and yellow fever virus) (Lee et al., 2000; Stocks and Lobigs, 1998) and was also successfully employed in the construction of a self-replicating, but noninfectious, tick-borne encephalitis virus genome containing a large truncation in the C protein (Kofler et al., 2004).

Preservation of sequential proteolytic processing of C and prM proteins is critically important for flavivirus replication, given that mutations in the c-region of the prM signal peptide, which uncoupled cleavage coordination, were detrimental for virus growth: while lethal in the case of yellow fever virus (Lee et al., 2000), they gave rise to budding mutants of MVEV, which displayed greatly increased release of nucleocapsid-free virus-like particles (VLPs) at the expense of virion production (Lobigs and Lee, 2004). Based on these findings, we have proposed a model for flavivirus morphogenesis, which posits that the inefficient signalase cleavage of prM promotes efficient nucleocapsid incorporation into budding flaviviral membranes. A

* Corresponding author. Emerging Pathogens and Vaccines Program, John Curtin School of Medical Research, The Australian National University, P.O. Box 334, Canberra, ACT 2601, Australia. Fax: +61 2 6125 2595.
E-mail address: Mario.Lobigs@anu.edu.au (M. Lobigs).

0042-6822/$ – see front matter © 2010 Elsevier Inc. All rights reserved.
doi:10.1016/j.virol.2010.02.008

caveat in this model was the observation that uncoupling of the coordinated cleavages at the C–prM junction by introduction of an "idealised" c-region into the prM signal peptide partially prevented cleavage of C protein. This was reflected in the accumulation of an anchC precursor (the C protein linked to the prM signal peptide) in mutant virus-infected cells (Lobigs and Lee, 2004). We hypothesised that additional mutations in the prM signal peptide would enhance NS2B-3 protease-catalysed cleavage of anchC and allow us to select a variant virus, in which both cleavages at the C–prM junction take place efficiently and independently of each other. Here, we identify a combination of substitutions in the prM signal peptide, which repair efficient cleavage of anchC, while maintaining uncoupled signalase cleavage of prM. In addition to the findings derived from the phenotypic characterisation of this mutant virus, we report that the presence of a cleavable transmembrane anchor of C protein enhances the assembly efficiency of MVEV replicon particles in packaging cell lines ectopically expressing the viral structural proteins.

Results

Mutagenesis of the prM signal peptide

To generate a C–prM junction where both cleavages occur efficiently and independently of each other, various amino acid changes were introduced into the prM signal peptide, in addition to the PQAQA mutation. Four categories of mutations were tested (Fig. 1): (i) the hydrophobicity of the n-region of the signal peptide was increased (mutants P + E109I and P + E109I + T110V + S111L), given that introduction of the PQAQA mutation into the yellow fever virus prM signal peptide was lethal for virus production but selected for viable viruses with second-site mutations involving mostly the substitution of polar or charged amino acids in the n-region of the signal peptide with hydrophobic residues (Lee et al., 2000); (ii) tryptophane residues were introduced N-terminal to the c-region of the signal peptide to prevent putative slippage of the transmembrane segment after signalase cleavage (mutant P + T100W + S111W), given the strong preference of tryptophane as flanking residue of transmembrane segments for location near the lipid–water interface, thereby stabilising the positioning of the signal peptide in the membrane (Killian and von Heijne, 2000); (iii) the n-region of the prM signal peptide was lengthened by insertion of one or two uncharged polar residues (mutants P + 1aa and P + 2aa); and (iv) 10 amino acids were inserted into the n-region of the signal peptide (P + 10aa) to produce a sequence of 14 residues identical to that at the N-terminus of the MVEV NS5 protein, which is cleaved efficiently from the upstream NS4B protein by the NS2B-3 protease (Lobigs, 1992).

We have shown previously that introduction of the PQAQA mutation into the MVEV genome is deleterious but not lethal for MVEV replication (Lobigs and Lee, 2004). To investigate if growth of the PQAQA mutant virus could be enhanced by the additional changes in the prM signal peptide aimed at improving cleavage of anchC, virus recovery following electroporation of BHK cells with full-length RNA transcripts was compared relative to WT and PQAQA mutant. Transfection with in vitro-synthesised rMVEV.P + E109I, rMVEV.P + 1aa, and rMVEV.P + 2aa RNAs allowed recovery of virus, while the other constructs did not produce viable virus (Fig. 1). The plaques produced by rMVEV.P + E109I were markedly smaller than those for variants rMVEV.P + 1aa and rMVEV.P + 2aa, and those for the latter two variants were comparable in size to MVEV.PQAQA plaques but clearly smaller than the rMVEV plaques (Fig. 1). This indicated that the additional mutations introduced into the PQAQA prM signal peptide were either detrimental or failed to significantly enhance virus growth relative to that of rMVEV.PQAQA.

In vivo selection of a PQAQA signal peptide variant with enhanced virus growth

Variants with P + E109I, P + 1aa, or P + 2aa mutations showed heterogeneous plaque sizes on Vero cells following virus amplification. Plaque isolates were sequenced in the C–prM gene region with results shown in Table 1. Analysis of 6 isolates of rMVEV.P + E109I showed two revertant genotypes, where, in each case, an A125V reversion at the −1 residue of the prM signalase cleavage site was observed. This mutation in the PQAQA motif was previously reported to restore the coordinated cleavages at the C–prM junction (Lobigs and Lee, 2004). Similarly, the P121L mutation in the PQAQA motif identified in two revertants with large plaque phenotype (4–5 mm) derived from rMVEV.P + 1aa was previously found to repair the sequential order of cleavages between C and prM proteins (Lobigs and Lee, 2004). These revertants were not further analysed, given that the

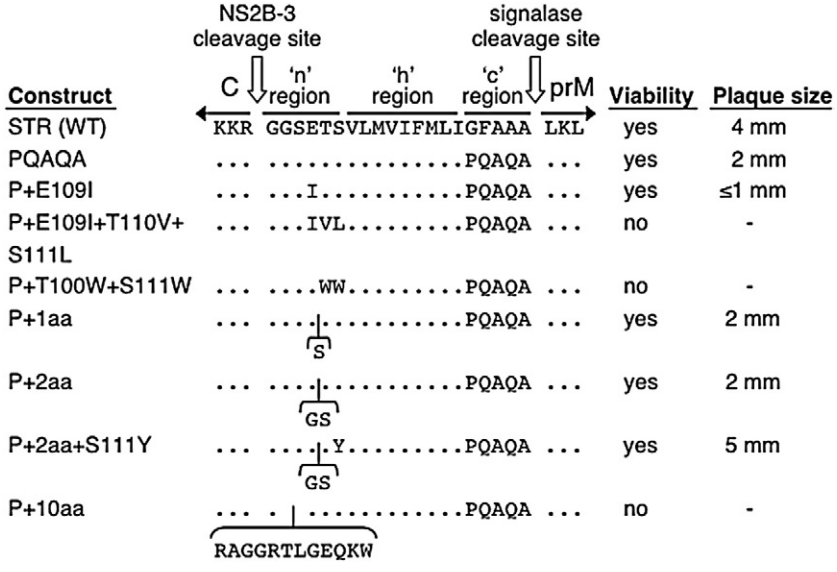

Fig. 1. Mutations introduced into the prM signal peptide. The MVEV prM signal peptide at the C–prM junction with cleavage sites and sequences we consider the n-, h-, and c-regions is shown at the top. Substitutions and insertions introduced into this region and designation of the mutant constructs are given below. Residues, which are unchanged relative to WT, are denoted by dots. The viability of infectious clone-derived mutant viruses and the corresponding plaque sizes on Vero cell monolayers stained with neutral red on day 4 pi and recorded the following day are given.

Table 1
Recovery of pseudo-reversions and compensatory mutations.

Variants (bold) and pseudoreversions/compensatory mutations acquired[a]	No. of times isolated	Amino acid change[b] (nucleotide change)
rMVEV.P + E109I		
Revertant 1	3	$Ile_{109} \rightarrow Thr$ (ATA → ACA) $Ala_{125} \rightarrow Val$ (GCC → GTC)
Revertant 2	3	$Ala_{125} \rightarrow Val$ (GCC → GTC)
rMVEV.P + 1aa		
Revertant 3	2	$Pro_{121} \rightarrow Leu$ (CCA → CTA)
Variant 1 (V1)	1	$Gln_{556} \rightarrow Leu$ (CAA → CTA)[c]
rMVEV.P + 2aa		
Variant 2 (V2)	1	$Ser_{111} \rightarrow Tyr$ (TCC → TAC) $Glu_{529} \rightarrow Lys$ (GAA → AAA)[d]

[a] Infectious clone-derived variants were amplified and plaque-purified on Vero cells.
[b] Amino acid numbering from the first residue in the C protein.
[c] Codon 264 in E protein.
[d] Codon 237 in E protein.

aim of this investigation was to isolate a virus in which the two cleavages at the C–prM junction are efficient but take place independently of each other.

A second rMVEV.P + 1aa plaque isolate (plaque size: 2–3 mm) showed the expected sequence at the C–prM junction, and subsequent sequencing of the E genes uncovered a Q556L substitution at codon 264 in the E protein (rMVEV.P + 1aa/V1; Table 1). A large plaque variant derived from rMVEV.P + 2aa showed an additional mutation in the prM signal peptide (S111Y) and a change at residue 237 (E529K) in E protein (Table 1). Notably, the plaque size of this variant (rMVEV.P + 2aa/V2) was larger than that of WT virus (Fig. 1), and the PQAQA motif and 2 amino acid insertion in the prM signal peptide were intact.

Capsid cleavage of prM signal peptide mutant viruses

Radioimmunoprecipitation with a C protein-specific antiserum from rMVEV-infected cell lysates recovered the C protein band (~14.5 kDa), whereas rMVEV.PQAQA-infected cell lysates yielded two bands of similar intensity, which correspond to C and anchC (Fig. 2A, lanes 1 and 2, respectively) (Lobigs and Lee, 2004). In variant rMVEV.P + 2aa/V2, efficient cleavage of C protein was restored, based on recovery of only authentic C in the absence of detectable anchC protein in the immunoprecipitation (Fig. 2A, lane 3).

To determine which of the second-site mutations in the structural polyprotein region acquired by variant rMVEV.P + 2aa/V2 accounted for restoration of efficient C cleavage, the S111Y and E529K mutations were introduced individually or combined into the P + 2aa background. The S111Y mutation was critical for efficient C protein cleavage, while the E529K change did not enhance cleavage (Fig. 2A, lanes 6 and 7, respectively). The presence of both pseudoreversions in variant rMVEV.P + 2aa + S111Y + E529K also resulted in an efficient C cleavage phenotype (Fig. 2A, lane 8). Variant rMVEV.P + 1aa/V1 did not display markedly improved C protein cleavage relative to rMVEV.PQAQA (Fig. 2A, lane 9).

N-region changes in the prM signal peptide do not override efficient signalase cleavage in the presence of the PQAQA mutation

To ascertain that the mutations in the n-region of the prM signal peptide in rMVEV + 2aa/V2 did not downmodulate cleavage of prM and thereby restore dependence of the signalase cleavage on prior NS2B-3 protease-catalysed cleavage of C protein, viral protease-independent production of prM was evaluated in transient transfection experiments. As shown previously (Stocks and Lobigs, 1998), transfection of COS-7 cells with a plasmid encoding the WT MVEV structural polyprotein

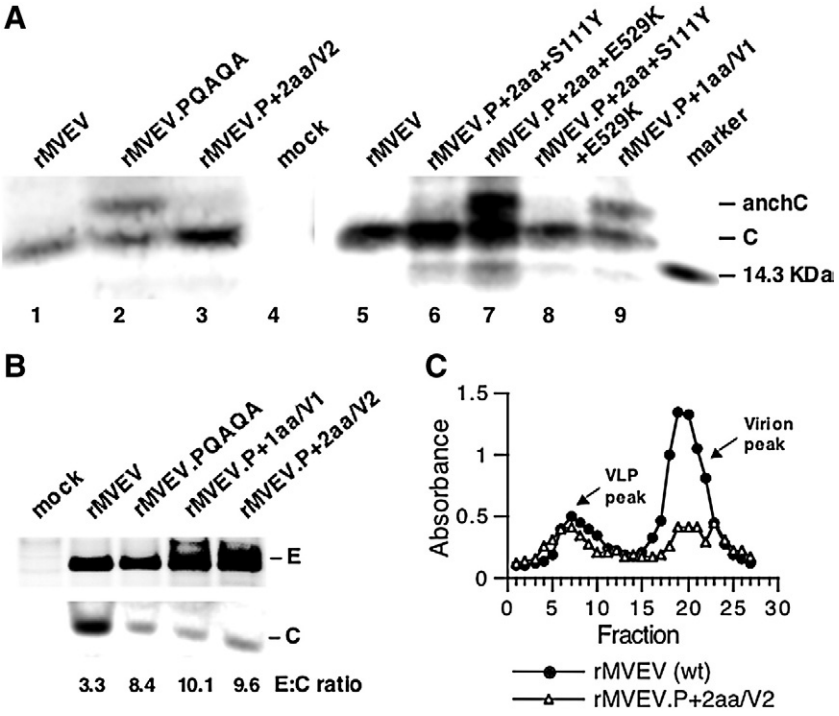

Fig. 2. Effect of mutations in the prM signal peptide on C protein cleavage and nucleocapsid incorporation into viral membranes. BHK cells were infected with rMVEV or variants (MOI ~5) or left uninfected. (A) At 18 h pi, the cells were metabolically labeled for 2 h. Immunoprecipitation was with an anti-C protein antiserum and proteins were subjected to SDS–PAGE (15% acrylamide). Bands corresponding to C and anchC are labeled, and the position of a 14.3-kDa marker protein is indicated. (B) Cell monolayers were metabolically labeled from 18 to 24.5 h pi, the culture supernatant was clarified by centrifugation, and particulate material was recovered by PEG precipitation. The secreted products were analysed by SDS–PAGE (15% acrylamide), and bands corresponding to the E and C proteins are shown. To calculate E/C protein ratios, the radioactivity in the corresponding bands was quantitated as photostimulated luminescence using the PhosphorImager scans, and values were divided by the number of Met and Cys residues present in E (21) and C proteins (5). (C) Vero cell-grown rMVEV and rMVEV.P + 2aa/V2 (2×10^7 and 1×10^7 PFU, respectively) were subjected, in parallel, to centrifugation on 10% to 30% sucrose density gradients, and the E protein content in fractions collected from the top of the gradients was determined using a capture ELISA.

(pSTR) resulted in production of only a small amount of prM and the presence of a C–prM precursor band in the absence of C protein cleavage (Figs. 3A and B), while cotransfection of pSTR with a plasmid encoding the viral NS2B-3 protease (pNS3/T) resulted in cleavage of C protein (Fig. 3B), thereby triggering signalase cleavage of prM (Fig. 3A). In the presence of the PQAQA mutation, signalase cleavage of prM took place efficiently in the absence of the viral protease (Fig. 3A), while anchC protein was immunoprecipitated with a C protein-specific antiserum; anchC was not detectably cleaved to mature C protein by the NS2B/3 protease (Fig. 3B). Efficient viral protease-independent cleavage of prM due to the presence of the PQAQA mutation was not abrogated as a consequence of additional mutations (P + 2aa + S111Y) in the n-region of the signal peptide, which was also reflected in the absence of a C–prM precursor band (Fig. 3).

Coexpression of the viral protease in cells transfected with the P + 2aa + S111Y mutant plasmid showed evidence of partial processing of anchC to authentic C protein (Fig. 3B). However, given that a band marginally smaller than the C protein was consistently precipitated from lysates of cells transfected with this and also the PQAQA construct in the absence of coexpression of the NS2B-3 protease, the data were ambiguous. A discrepancy in C protein cleavage efficiency in virus infected relative to transiently transfected cells has been observed previously for the PQAQA mutant and pseudorevertants thereof (Lobigs and Lee, 2004), suggesting that trans-cleavage of anchC in transfected cells is less efficient than cleavage in *cis* during virus infection.

Uncoupling of the coordinated cleavages at the C–prM junction results in inefficient virion assembly

Fig. 2A showed that efficient anchC cleavage was restored in rMVEV.P + 2aa/V2 infected cells, while rMVEV.PQAQA and rMVEV.P + 1aa/V1 displayed an inefficient anchC cleavage phenotype. Despite this difference in anchC cleavage, each of the mutant viruses showed markedly poorer assembly efficiency relative to rMVEV based on the comparison of E relative to C protein content of particles released from virus-infected BHK cells during a 6.5-h metabolic labeling interval (Fig. 2B). This result was consistent with our earlier observation for rMVEV.PQAQA showing an increased release of VLPs at the expense of that of virion particles (Lobigs and Lee, 2004). Flavivirus VLPs consist of prM and E protein-modified membranes but lack a nucleocapsid (Smith et al., 1970; Stollar, 1969), and the virion/VLP ratio of a virus preparation is a measure of assembly efficiency. A marked difference in virion/VLP content in Vero cell-grown rMVEV and rMVEV.P + 2aa/V2 was observed after sucrose gradient centrifugation (Fig. 2C), consistent with the poorer assembly efficiency of the mutant virus relative to the parent.

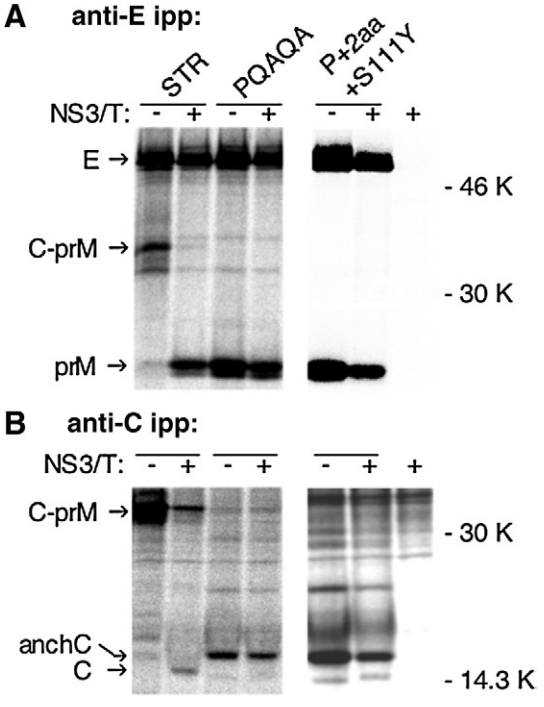

Fig. 3. Effect of mutations in the prM signal peptide on prM cleavage. COS-7 cells were transfected with WT or mutant expression plasmids encoding the MVEV structural polyproteins in the absence (−) or presence (+) of a plasmid (pNS3/T) encoding the NS2B-3 protease. At 2 days after transfection, the cells were metabolically labeled for 2 h, and products were immunoprecipitated from the lysates with an anti-E protein mAb (A) or a C protein-specific antiserum (B) and analysed by SDS–PAGE (12% acrylamide). Positions of E, C–prM, and prM (coprecipitated as a result of heterodimerisation with E) are labeled; the positions and sizes (in kilodaltons) of marker proteins are indicated.

Efficient flavivirus assembly requires a cleavable transmembrane anchor of C protein

To provide direct evidence for a role of C protein cleavage by the NS2B-3 protease in virus morphogenesis, a replicon particle assembly assay was established, which uses ectopic expression of the MVEV structural proteins in stably transfected cells for replicon particle production following introduction of MVEV replicon RNA into cells. Four packaging cell lines were generated (Fig. 4A): C–prM–E cells inducibly express the authentic structural polyprotein region of MVEV; C.IRES–prM–E cells express the same region, but with a termination codon after the C-terminal amino acid of C protein, followed by an EMCV IRES for translation of the prM and E protein; in anchC.IRES–prM–E cells, a termination codon and the IRES were inserted downstream of anchC and the prM signal peptide for translocation of the prM protein was duplicated; in C–pr.IRES–prM–E cells, a termination codon, the IRES and the duplicated prM signal peptide were inserted at the furin cleavage site in prM (pr–M junction). Expression of the predicted MVEV polypeptides shown in Fig. 4A was confirmed by pulse-labeling and radioimmunoprecipitation with C and E protein-specific antibodies (data not shown).

To investigate packaging competence of an MVEV replicon in the different cell lines, replicon spread was first investigated by flow cytometry and staining with an NS1 protein-specific antibody (Fig. 4B). While at 2 days pi with replicon particles only a minor proportion of cells (<5%) showed NS1-specific staining, replicon spread was clearly apparent at 4 days pi in cell monolayers expressing the C–prM–E, C.IRES–prM–E and C–pr.IRES–prM–E polyproteins, but not in anchC.IRES–prM–E or 293 control cells. Accordingly, the expression of anchC did not support replicon particle production, in contrast to expression of mature C protein or the C–pr polypeptide (which requires NS2B-3 mediated cleavage of C) in addition to the prM and E proteins from separate coding units.

For quantitation of assembly efficiency in the packaging-competent cell lines, replicon particle release was measured by real-time qRT–PCR. E protein expression from 5′cap- or IRES-driven translation was comparable in the 3 cell lines at 4 days after induction with tetracycline and infection with replicon particles (Fig. 4C). Replicon particle release from C–pr.IRES–prM–E cells exceeded that from C.IRES–prM–E cells by 23-fold at 2 days pi and ~5-fold at later time points, demonstrating that a cleavable membrane-anchored form of C protein markedly improved particle production relative to expression of mature C protein (Fig. 4D). Replicon particle release was most efficient from the packaging cell line expressing the C–prM–E polyprotein region from a single coding unit.

Growth of prM signal peptide variants in mammalian cells

Given the defect in virion assembly associated with mutations introduced into the prM signal peptide that uncouple the cleavage

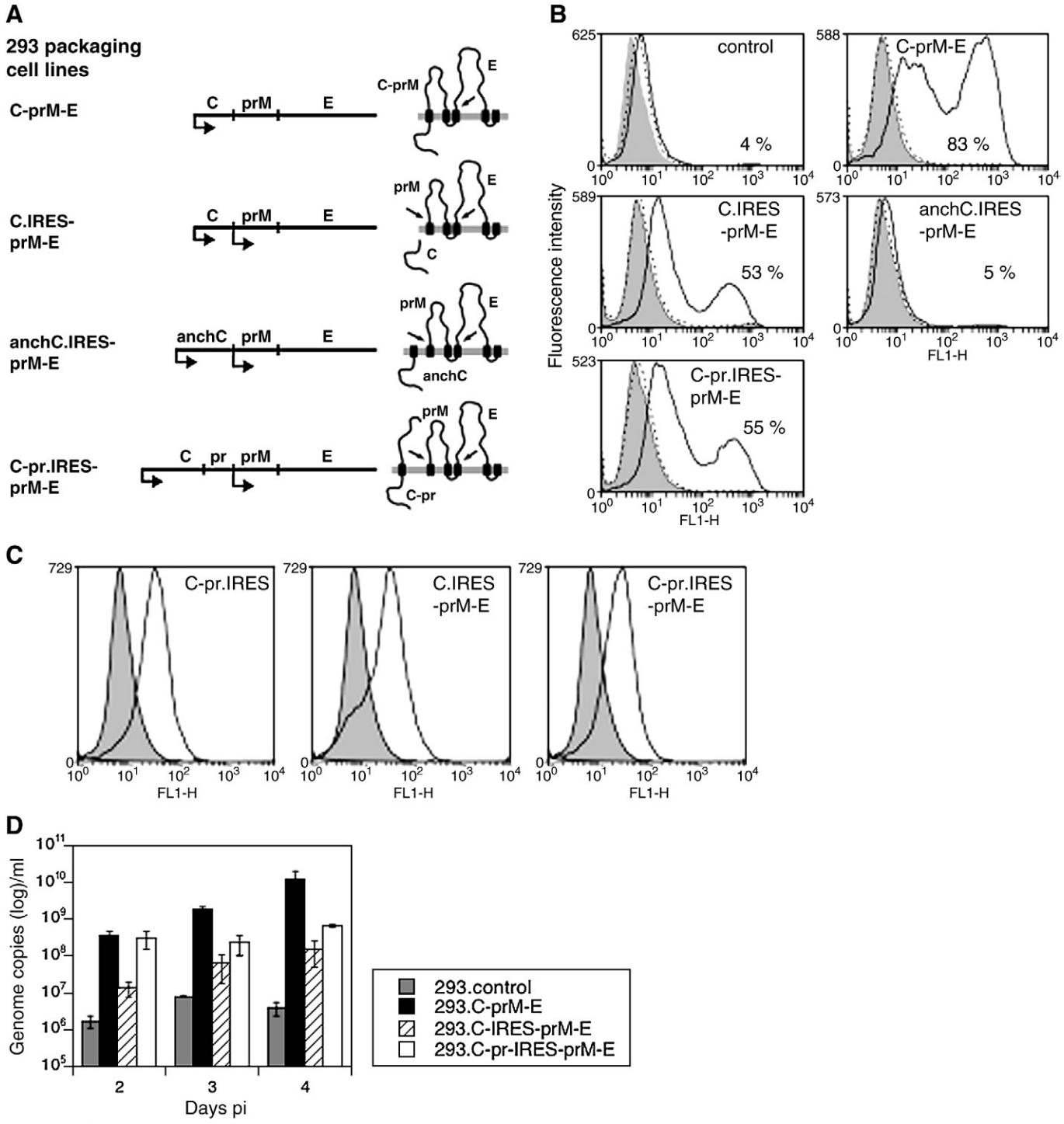

Fig. 4. Efficient MVEV replicon packaging requires the cleavable transmembrane anchor of C protein. (A) Schematic diagram showing the MVEV polyprotein regions encoded under a tetracycline-inducible promoter in the 293 packaging cell lines. Arrows indicate the 5′cap- and IRES-driven translation start sites. The putative membrane topology of the translation products is indicated on right, with solid bars representing transmembrane domains and ER luminal and cytoplasmic location above and below the shaded line, respectively, and diagonal arrows depict signal peptidase cleavages. (B) Flow cytometry histograms showing NS1 protein-specific staining in uninfected (shaded histogram) and MVEV replicon-infected cells at 2 days pi (broken line) and at 4 days pi (solid line). The numbers indicate the percentages of NS1-positive cells. (C) Flow cytometry histograms showing E protein-specific staining in uninduced (shaded histogram) and induced (solid line) cells at 4 days pi. (D) Real-time qRT–PCR quantitation of replicon particle-associated RNA in culture supernatants of 293 control or packaging cell lines infected with MVEV replicon particles and induced with tetracycline over a 4-day period. Error bars indicate the SEM of two qRT–PCR determinations for each sample shown. The data are representative of 3 independent experiments.

coordination at the C–prM junction, an adverse impact of these mutations on virus growth was anticipated. Surprisingly, rMVEV.P + 2aa/V2 showed comparable growth relative to rMVEV in 3 mammalian cell lines in terms of kinetics and plateau virus titers achieved (Fig. 5A). In contrast, growth of rMVEV.P + 1aa/V1 in Vero, K562, and HepG2 cells was ~10-fold poorer in comparison to WT virus but markedly improved in Vero cells relative to rMVEV.PQAQA (Fig. 5A). Growth of the latter virus in K562 and HepG2 cells was not tested. Furthermore, quantitation of virion-associated viral RNA release from infected Vero cells by real-time qRT–PCR confirmed that packaging of viral RNA into secreted viral particles was equally efficient between rMVEV and rMVEV.P + 2aa/V2 (Fig. 5B). Release of virion-associated

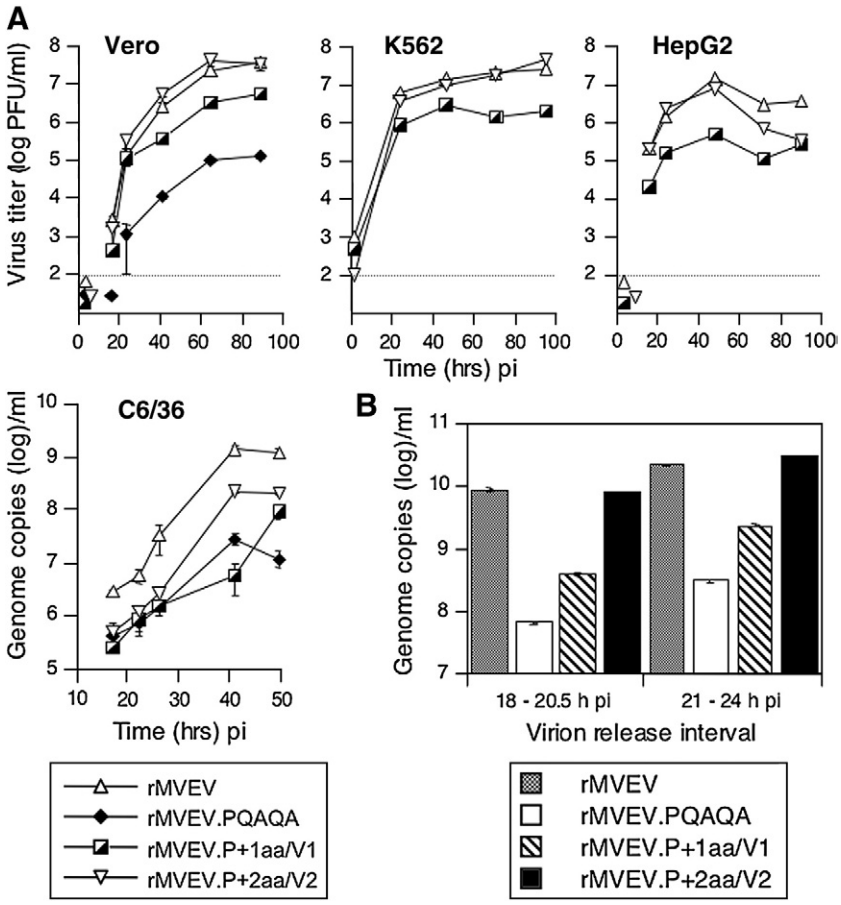

Fig. 5. Growth of rMVEV and prM signal peptide variants in mammalian and insect cells. (A) Vero, K562, HepG2, and mosquito C6/36 cells were infected at multiplicities of 0.02, 0.04, 0.1, and 0.2, respectively. Infectivity of the virus stocks for the different cell lines was determined by flow cytometry at 18 h pi or 24 h pi in case of C6/36 cells, using a mAb specific for NS1 protein. Virus titers in growth samples were measured by plaque assay on Vero cells (growth curves in Vero, K562, and HepG2 cells) or real-time qRT–PCR (growth curves in C6/36 cells). Dotted lines denote detection limit of virus yield by plaque assay. (B) Real-time qRT–PCR quantitation of virion particle-associated RNA release into the culture supernatant of infected Vero cells (MOI ~0.5) during time intervals, as indicated. Error bars indicate the SEM of 2 qRT–PCR determinations for each sample shown.

RNA from rMVEV.PQAQA- and rMVEV.P + 1aa/V1-infected Vero cells was reduced by 100- and 10-fold, respectively, relative to WT virus-infected cells and consistent with the results of the growth assay. Taken together, these data suggest that cleavage of anchC, which is efficient in rMVEV.P + 2aa/V2, but incomplete in rMVEV.PQAQA- and rMVEV.P + 1aa/V1-infected cells (Fig. 3A), is critically important for virus growth in mammalian cells. Surprisingly, the reduced assembly efficiency of rMVEV + 2aa/V2 relative to parent virus did not noticeably impact on growth in mammalian cell culture.

Growth of prM signal peptide variants in mosquito cells

Mosquito C6/36 cells differed from the mammalian cell lines in permissiveness to growth of the prM signal peptide mutants relative to rMVEV (Fig. 5A). The more pronounced detrimental impact of the PQAQA mutation in the prM signal peptide on MVEV growth in C6/36 in comparison to Vero cells was noted previously (Lobigs and Lee, 2004). The additional changes in the prM signal peptide in rMVEV.P + 2aa/V2 improved growth of the variant in mosquito cells but not to the level of rMVEV, which was ~10-fold more efficient than that of the variant. The growth in C6/36 cells of rMVEV.P + 1aa/V1 was not markedly enhanced relative to that of rMVEV.PQAQA (Fig. 5A).

Only partial cleavage of anchC was found in rMVEV.P + 2aa/V2-infected C6/36 cells grown at 28 °C (Fig. 6A), in contrast to complete cleavage seen in BHK cells (Fig. 2A). This observation could explain the poorer growth of the variant in C6/36 cell maintained at 28 °C, in comparison to rMVEV. However, when cultured at 37 °C, cleavage of anchC in rMVEV.P + 2aa/V2-infected C6/36 cells was markedly enhanced (Fig. 6A), and growth of this variant was comparable to that of rMVEV (Fig. 6B). AnchC cleavage for rMVEV.P + 1aa/V1 remained inefficient in C6/36 cells grown at 37 °C as did the growth phenotype of this variant. This result provides a further demonstration for the critical role of anchC cleavage in virus growth.

Effect of uncoupling of the coordinated cleavages at the C–prM junction on virus growth and virulence in mice

Virulence and pathogenesis of rMVEV.P + 2aa/V2 in mice was significantly attenuated relative to rMVEV. While inoculation, i.p., of 10^2 and 10^3 PFU of rMVEV into 3-week-old mice was 100% lethal, as has been shown previously (Lobigs et al., 1988), the same doses of the mutant virus gave only 20% and 33% mortality, respectively ($P = 0.001$; Fig. 7A). Low-dose infection, i.v., of adult type I interferon response defective mice, which are a highly susceptible mouse model for flaviviral encephalitis (Lee et al., 2004; Lobigs et al., 2003; Samuel and Diamond, 2005), was 100% lethal for both viruses (Fig. 7B), although a significant difference in the average survival time was observed (rMVEV: 5.2 days, rMVEV.P + 2aa/V2: 7.9 days; $P = 0.002$). Growth of rMVEV.P + 2aa/V2 in IFN-α-R−/− mice was significantly attenuated relative to rMVEV (Fig. 7B), given that viremia at day 2 pi was reduced by ~10-fold ($P = 0.006$).

Discussion

Two cleavages at the flavivirus C–prM junction take place in a sequential order where cytosolic processing of C protein by the viral

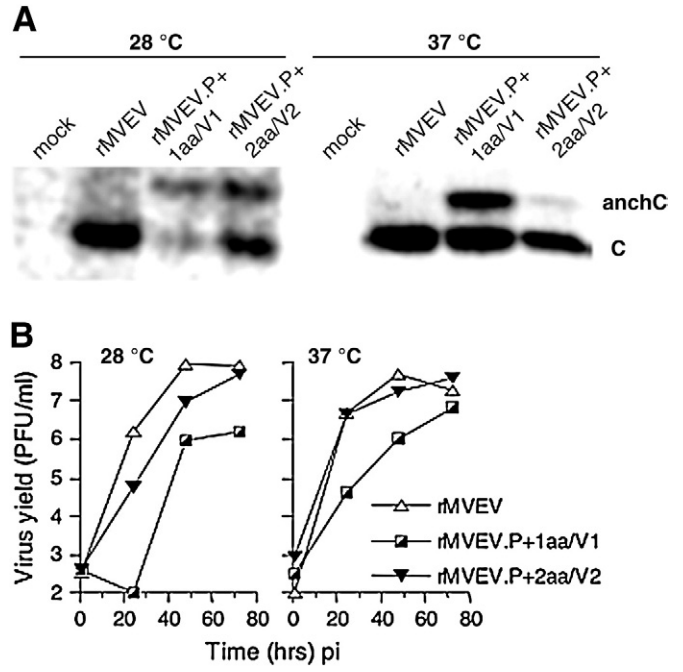

Fig. 6. Temperature dependence of anchC cleavage in C6/36 cells and impact on growth. (A) C6/36 cells were infected with rMVEV or variants (MOI ~0.5) followed by incubation at 28 °C or 37 °C for 48 h before the cells were metabolically labeled for 1.5 h. Immunoprecipitation was with an anti-C protein antiserum, and proteins were subjected to SDS–PAGE (15% acrylamide). Bands corresponding to C and anchC are labeled. (B) Cells were infected as above and incubated at 28 °C or 37 °C. Virus titers in growth samples were measured by plaque assay on Vero cells.

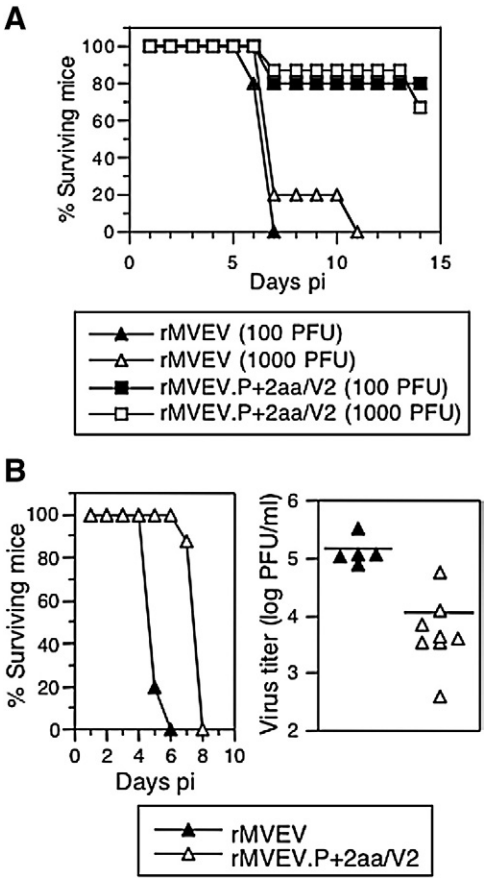

Fig. 7. Virulence in 3-week-old BALB/c and IFN-α-receptor knockout mice. (A) Groups of 3-week-old BALB/c mice ($n=5$, except group rMVEV.P + 2aa/V2 [1000 PFU], where $n=6$) were infected, i.p., and morbidity and mortality were recorded daily for a period of 21 days. (B) Six-week-old IFN-α-R−/− mice were infected, i.v., with 100 PFU of rMVEV ($n=5$) or rMVEV.P + 2aa/V2 ($n=8$) and morbidity and mortality were recorded daily. At 2 days pi, serum was collected and frozen at −70 °C. Viremia titers were determined by plaque assay on Vero cells. Each symbol represents an individual mouse, and mean titers are indicated by a horizontal line.

NS2B-3 protease triggers efficient ER luminal signalase cleavage of prM protein (Amberg et al., 1994; Amberg and Rice, 1999; Lee et al., 2000; Lobigs and Lee, 2004; Stocks and Lobigs, 1995, 1998). The prM signal peptide is pivotal in controlling this sequential accessibility of both cleavage sites to their respective proteases. Thus, when coordination of the cleavages was uncoupled by substitutions introduced into the c-region of the signal peptide to allow efficient prM cleavage, an anchC product with poor substrate properties for the NS2B-3 protease was generated (this study and Lobigs and Lee, 2004). Additional insertion of a dipeptide (Gly-Ser) plus selection of a compensatory mutation (S111Y) in the n-region of the prM signal peptide markedly improved proteolytic processing of anchC. We did not investigate the relative contribution of the two n-region changes on the PQAQA mutant background to the enhanced accessibility of the cleavage site in anchC to the viral protease. However, given that, in the absence of the dipeptide insertion, propagation of a PQAQA variant of MVEV selected almost exclusively for reversions in the PQAQA mutation (Lobigs and Lee, 2004), it is likely that both n-region changes played a role. Accordingly, by the introduction of multiple changes into the prM signal peptide we have generated a mutant flavivirus in which signalase and NS2B-3 protease cleavages at the C–prM junction occurred efficiently and independently of each other. Phenotypic studies on this virus have provided insight into the physiological role of this unique mechanism for the regulation of the proteolytic processing events in the structural region of the flavivirus polyprotein.

We found that the cleavage of anchC was essential for the morphogenesis of MVEV. The replicon-packaging experiments demonstrated that the uncleaved form of anchC could not be utilised for assembly and release of replicon particles. Interestingly, trans-complementation of packaging of a yellow fever virus replicon was achieved in anchC-expressing cells, although assembly was more efficient in cells encoding C with the signal peptide and a stretch of the N-terminal amino acids of prM (Mason et al., 2006). This discrepancy from our results suggests virus-specific differences in accessibility of the anchC cleavage site to the viral protease. We also found a substantial reduction (≥10-fold) in virus growth in mammalian and mosquito cells infected with prM signal peptide mutant viruses that displayed partial cleavage of anchC, suggesting that either the reduced availability of mature C protein or an inhibitory effect of the presence of anchC on virion assembly was detrimental for virus growth. In addition, anchC has not been observed as a by-product of flavivirus replication. Taken together, these findings are consistent with the interpretation that efficient C protein cleavage is an essential outcome in modulation of the processing events between the C and prM proteins.

Given the importance of efficient C protein cleavage in flavivirus assembly, the question arises why this cleavage site has not evolved such that its accessibility to the viral protease is independent of the potentially inhibitory effect of downstream prM cleavage. The mutational analysis in the present study confirmed this possibility and was consistent with a recent study, which showed that viral protease-mediated cleavage of C protein was not essential for flavivirus replication, if liberation from the viral polyprotein was ascertained by introduction of the autocatalytic foot-and-mouth disease virus NS2A protein (Schrauf et al., 2009). However, in contrast to the approaches applied by us yielding authentic C protein, that of Schrauf et al. gave rise to a C-terminal 18-amino acid extension of C thereby preventing distinction between the contribution of

altered C protein structure and uncoupling of cleavage coordination at the C–prM junction on the deficient growth phenotype of their mutants relative to WT viruses. Previously, we have suggested that the sequential order of cleavages at the C–prM junction enhances nucleocapsid uptake into budding flaviviral membranes (Lobigs and Lee, 2004), an event which is apparently not driven by interactions between the nucleocapsid and cytoplasmic domains on the viral membrane proteins (Kuhn et al., 2002; Zhang et al., 2003). Here, we provide proof that this is the case. Using two replicon-packaging cell lines, which differ by the presence or absence of a cleavable transmembrane anchor of C protein, we show that replicon particle formation is markedly enhanced when NS2B-3 protease-mediated cleavage of C protein is required. It remains unclear why a cleavable, membrane-anchored form of C protein is a preferred component for initiation of flavivirus assembly rather than the mature C protein. We speculate that the former may be beneficial for initiation of nucleocapsid formation in a process putatively involving the interaction of membrane-anchored C protein with genomic RNA and/or oligomerisation with other C proteins. Alternatively, attraction of the NS2B-3 protease to the budding site could play a complementary role in virus assembly other than in the cleavage of C protein, given that the protease may be complexed with other viral or host components that could promote this process. Consistent with this interpretation, it has been noted that coupling between RNA replication and packaging is important for infectious flavivirus particle production (Khromykh et al., 2001; Liu et al., 2002; Pijlman et al., 2006) and that the helicase domain of NS3 plays an essential role in genome packaging and virus assembly, independently of its enzymatic function (Patkar and Kuhn, 2008).

Others have shown that flavivirus replicon particle assembly can take place when the C and prM-E proteins are translated from separate coding units (Gehrke et al., 2003; Khromykh et al., 1998; Orlinger et al., 2006). However, higher replicon-packaging efficiencies in trans-complementing cell lines were generally observed when the structural proteins were expressed as a single polyprotein (Harvey et al., 2004; Mason et al., 2006; Scholle et al., 2004). This was also noted in the present study, which showed that MVEV replicon particle production in 293 C–prM–E cells was optimal in comparison to packaging cells with bicistronic expression of C and prM–E proteins. Accordingly, at least two factors may contribute to the more efficient replicon-packaging in C–prM–E trans-complementation: (i) presence of a cleavable transmembrane domain of C protein, as discussed above, and (ii) retention of the viral transmembrane proteins, prM and E, at the assembly site, which is subject to regulation by the cleavages at the C–prM junction, and the concomitant reduction in their secretion in the form of VLPs.

A second key finding of this study was the remarkable insensitivity of flavivirus growth in cell culture to an assembly defect involving efficient nucleocapsid uptake into budding viral membranes. Thus, measurements of C protein incorporation into particles secreted from virus infected cells and virion/VLP ratios showed a markedly poorer assembly efficiency of variant, rMVEV.P + 2aa/V2, in comparison to WT virus. Nevertheless, growth of the two viruses in mammalian and mosquito cells (when cultured at 37 °C to ascertain efficient anchC cleavage) was indistinguishable. This result was unexpected and suggested that availability of the structural proteins at the site of virus morphogenesis in mutant virus-infected cells was not rate-limiting for infectious virion release. It is indicative of a substantial amount of wastage of virion component during growth of flaviviruses in cell culture. Interestingly, growth and virulence of rMVEV.P + 2aa/V2 in mice was attenuated relative to rMVEV, demonstrating the greater sensitivity of animal models to the reduced efficiency of virus assembly than found in cell culture. The latter confirms a physiological relevance for the obligatory sequence of cleavages at the C–prM junction, which may also apply to flavivirus replication in the arthropod vector.

Materials and methods

Cells

African green monkey kidney (Vero), baby hamster kidney (BHK), human erythroleukemia (K562), human liver carcinoma (HepG2), and *Aedes albopictus* (C6/36) mosquito cells were obtained from the American Type Culture Collection (ATCC). Vero, BHK, COS-7, and HepG2 cells were maintained at 37 °C in minimal essential medium (MEM; Gibco) supplemented with nonessential amino acids and 5% fetal bovine serum (FCS). K562 cells were maintained at 37 °C in RPMI medium supplemented with 10% FCS, and C6/36 cells were grown at 28 °C in MEM supplemented with nonessential amino acids and 10% FCS.

Virus

Infectious clone-derived rMVEV was used (Lee and Lobigs, 2000). Virus titration by plaque assay on Vero cells was performed as described (Licon Luna et al., 2002).

Eukaryotic expression plasmids

Plasmid pSTR designates an expression plasmid (pcDNA1; Invitrogen) encoding MVEV cDNA for the 5′UTR, C, prM and E genes plus 11 N-terminal codons of NS1. Plasmid pPQAQA is identical to pSTR except for substitutions in the c-region of the prM signal peptide that introduce the PQAQA mutation, as described (Stocks and Lobigs, 1998). Plasmid pNS3/T contains MVEV cDNA encoding 31% NS2A through to NS5 genes with an amber termination codon at the NS3–4A junction (Lobigs, 1992). To incorporate mutations into the prM signal peptide, fusion PCR using pPQAQA template DNA and appropriate oligonucleotides was performed as described (Lee and Lobigs, 2008). Mutagenised PCR products were ligated as 521-bp *Hind*III fragments into pPQAQA, replacing the corresponding WT cDNA regions. COS-7 cell transfection with expression plasmids was by the DEAE–dextran method (Lobigs, 1992).

Replicon-packaging cell lines

Stably transfected human embryonic kidney (293) cells for tetracycline-inducible expression of MVEV C, prM and E genes were constructed using the Flp-In T-Rex approach (Invitrogen) as recommended by the supplier. 293 C–prM–E cells encode the MVEV structural polyprotein region plus 11 N-terminal codons of NS1. 293 C.IRES–prM–E cells encode the same polyprotein region but with an amber termination codon at the 3′ end of the C gene, followed by the encephalomyocarditis virus (ECMV) IRES, which was amplified by PCR from plasmid pKUNrep4 (Varnavski et al., 2000). This allows 5′ cap-driven translation of authentic C protein and IRES-driven translation of the prM signal peptide (plus 3 N-terminal amino acids [Met-Val-Arg]), prM and E. In 293 anchC.IRES–prM–E and C–pr.IRES–prM–E cells, amber stop codons were inserted downstream of the cDNA for the prM signal peptide or at the junction of the pr and M genes, respectively, and followed by an IRES–prM–E gene cassette. Ectopic protein expression was induced by the addition of tetracycline (1 μg/ml) to the growth medium (DMEM [high glucose] supplemented with 10% FCS, blasticidin [15 μg/ml], and hygromycin B [200 μg/ml]).

MVEV replicon and replicon-packaging

A plasmid (pMVEV-rep) was generated from the MVEV full-length cDNA clone, pMVE-FL-v2 (see below), by deleting a cDNA region encompassing most of C, prM, and E proteins from residue 28 in C protein to residue 480 in E protein by digestion with the restriction enzymes *Spe*I and *Mun*I and religation. A serine codon (TCG) was

introduced at the junction of the truncated C and E proteins by site-directed mutagenesis to restore the correct reading frame. Replicon particle stocks were generated by electroporation of in vitro-transcribed replicon RNA into 293.C–prM–E cells as described (Lee and Lobigs, 2000), and culture of the cells for 8 days when the supernatant was harvested and stored in single-use aliquots at −70 °C. Titers in Vero cells of the MVEV replicon particle stocks were $\sim 5\times10^6$ infectious units/ml, when determined by flow cytometry performed at 24 h pi as described (Lee et al., 2006) using the NS1 protein-specific mAb, 4G4 (Clark et al., 2007), for the detection of replicon-infected cells. For the evaluation of replicon-packaging efficiency in the different 293 packaging cell lines, cell pellets (1.5×10^6 cells) were suspended in a 0.5-ml medium containing replicon particles (1.5×10^6 Vero cell infectious units) and incubated in a 37 °C incubator for 1 h with occasional vortexing. The cells were washed twice and maintained in 25-cm^2 cell culture flasks for up to 4 days using 5 ml of growth medium containing tetracycline (1 µg/ml), which was replenished daily.

Genome copy quantitation by real-time RT–PCR

Virion- or replicon particle-associated genome content in culture supernatants was measured by real-time RT–PCR. Culture supernatants (0.1 ml) were treated with RNase (20 µg/ml for 30 min at 37 °C) and RNA-extracted using Trizol (Invitrogen). Reverse transcription and real-time PCR were performed as described (Lee and Lobigs, 2008) using the downstream primer, 5′-AACTCCAAGAATCTGGCTCCCA-3′, and upstream primer, 5′-GGAAATGGTGGATGAGGAAAGG-3′. Each RNA sample was tested in duplicates,, and virion RNA content was determined by extrapolation from the standard curve generated within each experiment. Standards were in vitro-transcribed replicon RNA generated from pMVEV-rep, extracted with phenol–chloroform, and quantitated by spectrophotometry. The detection limit of the assay was 2×10^5 RNA copies/ml.

Full-length infectious MVEV cDNA clone

An infectious cDNA clone of MVEV has been described (Lee and Lobigs, 2000). In this study, a second version of this clone (pMVE-FL-v2) was used, which differed from the previous one by a silent mutation at nucleotide 4730 (T to C change) to remove an *Nsi*I site, plus an *Nsi*I site introduced at the 3′ end of the MVEV cDNA. Hence, digestion of the clone with *Nsi*I followed by blunt-ending with T4 DNA polymerase and in vitro transcription with T7 RNA polymerase allowed the generation of an RNA transcript, which differed at the 3′ terminus from the authentic MVEV RNA genome by the presence of only one additional nucleotide.

Sucrose gradient analysis and capture ELISA

Sucrose gradient centrifugation was as described (Lobigs and Lee, 2004). Fractions of ~0.4 ml each were collected from the top of the gradients, diluted 2- to 5-fold in PBS, and 50 µl was loaded onto 96-well microtiter plates coated with a rabbit anti-MVEV hyperimmune serum diluted 1:5000 in carbonate buffer. Following incubation for 2 h at 37 °C, plates were washed 3 times with PBS/T (PBS containing 0.05% Tween 20) and anti-E protein mAb 8E7 (1 µg) diluted in Blotto/Tween (5% nonfat dry milk, 0.2% Tween in PBS) was added. The plates were incubated for 2 h at 37 °C. Following 3 washes with PBS/T, 50 µl/well of horseradish peroxidase-conjugated goat anti-mouse immunoglobulin diluted 1:1000 in Blotto/Tween was added, and plates were incubated for 1 h at 37 °C. The wells were washed 5 times with PBS/T and once with dH_2O, and 50 µl/well of the peroxidase substrate ABTS was added, and the plates were kept at room temperature for ~20 min to allow colour development. Plates were read at 405 nm in a microplate reader.

Metabolic labeling, immunoprecipitation, and SDS–PAGE

Transient transfections of COS-7 cells with eukaryotic expression plasmids, metabolic labeling, and immunoprecipitations with E protein-specific mAb, 8E7 (Hall et al., 1990), or a C protein-specific antiserum (Lobigs and Lee, 2004) were as described (Stocks and Lobigs, 1998), and metabolic labeling experiments using infected BHK or C6/36 cells were performed as described (Lobigs and Lee, 2004), with the variation of addition of the proteasome inhibitor, MG132 (Sigma), to the starvation and labeling media (10 µM final concentration) to prevent degradation of C protein. For the recovery of virions and VLPs from the culture supernatants of infected and metabolically labeled BHK cells, polyethylene glycol (PEG) 8000 was used as described (Lobigs et al., 1986). The pellets were dissolved in Laemmli sample buffer and analysed by SDS–PAGE. SDS–PAGE gels were fixed for 30 min in 10% acetic acid and rinsed with water for 10 min, and dried gels were placed on a PhosphorImager plate for 2–3 days. The plates were scanned with a Fuji PhosphorImager. Photoshop images shown have been minimally manipulated.

Animal experiments

Virulence assays were performed in 3-week-old BALB/c mice by intraperitoneal (i.p.) inoculation of virus. The animals were observed twice daily for a period of 21 days. Interferon-alpha receptor knockout (IFN-α-R−/−) mice (Müller et al., 1994) were used at 6 weeks of age and infected with virus intravenously (i.v.). Serum samples were collected at 2 days pi to determine viremia levels by plaque assay on Vero cells. Mice were euthanized when signs of encephalitis were apparent.

Statistics

Difference in survival ratios in mouse challenge experiments was assessed using Fischer's exact test. The Wilcoxon signed-rank test was used to assess differences in viremia titers and average time to death for significance.

Acknowledgments

This work was supported by the National Health and Medical Research Council of Australia (project grants 224262 and 366736).

References

Amberg, S.M., Rice, C.M., 1999. Mutagenesis of the NS2B–NS3-mediated cleavage site in the flavivirus capsid protein demonstrates a requirement for coordinated processing. J. Virol. 73, 8083–8094.
Amberg, S.M., Nestorowicz, A., McCourt, D.W., Rice, C.M., 1994. NS2B-3 proteinase-mediated processing in the yellow fever virus structural region: in vitro and in vivo studies. J. Virol. 68, 3794–3802.
Clark, D.C., Lobigs, M., Lee, E., Howard, M.J., Clark, K., Blitvich, B.J., Hall, R.A., 2007. In situ reactions of monoclonal antibodies with a viable mutant of Murray Valley encephalitis virus reveal an absence of dimeric NS1 protein. J. Gen. Virol. 88, 1175–1183.
Gehrke, R., Ecker, M., Aberle, S.W., Allison, S.L., Heinz, F.X., Mandl, C.W., 2003. Incorporation of tick-borne encephalitis virus replicons into virus-like particles by a packaging cell line. J. Virol. 77, 8924–8933.
Hall, R.A., Kay, B.H., Burgess, G.W., Clancy, P., Fanning, I.D., 1990. Epitope analysis of the envelope and non-structural glycoproteins of Murray Valley encephalitis virus. J. Gen. Virol. 71, 2923–2930.
Harvey, T.J., Liu, W.J., Wang, X.J., Linedale, R., Jacobs, M., Davidson, A., Le, T.T., Anraku, I., Suhrbier, A., Shi, P.Y., Khromykh, A.A., 2004. Tetracycline-inducible packaging cell line for production of flavivirus replicon particles. J. Virol. 78, 531–538.
Khromykh, A.A., Varnavski, A.N., Westaway, E.G., 1998. Encapsidation of the flavivirus Kunjin replicon RNA by using a complementation system providing Kunjin virus structural proteins in trans. J. Virol. 72, 5967–5977.
Khromykh, A.A., Varnavski, A.N., Sedlak, P.L., Westaway, E.G., 2001. Coupling between replication and packaging of flavivirus RNA: evidence derived from the use of DNA-based full-length cDNA clones of Kunjin virus. J. Virol. 75, 4633–4640.
Killian, J.A., von Heijne, G., 2000. How proteins adapt to a membrane–water interface. Trends Biochem. Sci. 25, 429–434.

Kofler, R.M., Aberle, J.H., Aberle, S.W., Allison, S.L., Heinz, F.X., Mandl, C.W., 2004. Mimicking live flavivirus immunization with a noninfectious RNA vaccine. Proc. Natl. Acad. Sci. U. S. A. 101, 1951–1956.

Kuhn, R.J., Zhang, W., Rossmann, M.G., Pletnev, S.V., Corver, J., Lenches, E., Jones, C.T., Mukhopadhyay, S., Chipman, P.R., Strauss, E.G., Baker, T.S., Strauss, J.H., 2002. Structure of dengue virus: implications for flavivirus organization, maturation, and fusion. Cell 108, 717–725.

Lee, E., Lobigs, M., 2000. Substitutions at the putative receptor-binding site of an encephalitic flavivirus alter virulence and host cell tropism and reveal a role for glycosaminoglycans in entry. J. Virol. 74, 8867–8875.

Lee, E., Lobigs, M., 2008. E protein domain III determinants of yellow fever virus 17D vaccine strain enhance binding to glycosaminoglycans, impede virus spread, and attenuate virulence. J. Virol. 82, 6024–6033.

Lee, E., Stocks, C.E., Amberg, S.M., Rice, C.M., Lobigs, M., 2000. Mutagenesis of the signal sequence of yellow fever virus prM protein: enhancement of signalase cleavage In vitro is lethal for virus production. J. Virol. 74, 24–32.

Lee, E., Hall, R.A., Lobigs, M., 2004. Common E protein determinants for attenuation of glycosaminoglycan-binding variants of Japanese encephalitis and West Nile viruses. J. Virol. 78, 8271–8280.

Lee, E., Pavy, M., Young, N., Freeman, C., Lobigs, M., 2006. Antiviral effect of the heparan sulfate mimetic, PI-88, against dengue and encephalitic flaviviruses. Antiviral Res. 69, 31–38.

Licon Luna, R.M., Lee, E., Müllbacher, A., Blanden, R.V., Langman, R., Lobigs, M., 2002. Lack of both Fas ligand and perforin protects from flavivirus-mediated encephalitis in mice. J. Virol. 76, 3202–3211.

Lindenbach, B.D., Rice, C.M., 2001. *Flaviviridae*: the viruses and their replication, In: Knipe, D.M., Howley, P.M. (Eds.), Fields Virology, 4th ed. Lippincott Williams& Wilkins, Philadelphia, PA, pp. 991–1042.

Liu, W.J., Sedlak, P.L., Kondratieva, N., Khromykh, A.A., 2002. Complementation analysis of the flavivirus Kunjin NS3 and NS5 proteins defines the minimal regions essential for formation of a replication complex and shows a requirement of NS3 in *cis* for virus assembly. J. Virol. 76, 10766–10775.

Lobigs, M., 1992. Proteolytic processing of a Murray Valley encephalitis virus non-structural polyprotein segment containing the viral proteinase: accumulation of a NS3-4A precursor which requires mature NS3 for efficient processing. J. Gen. Virol. 73, 2305–2312.

Lobigs, M., 1993. Flavivirus premembrane protein cleavage and spike heterodimer secretion require the function of the viral proteinase NS3. Proc. Natl. Acad. Sci. 90, 6218–6222.

Lobigs, M., Lee, E., 2004. Inefficient signalase cleavage promotes efficient nucleocapsid incorporation into budding flavivirus membranes. J. Virol. 78, 178–186.

Lobigs, M., Marshall, I.D., Weir, R.C., Dalgarno, L., 1986. Genetic differentiation of Murray Valley encephalitis virus in Australia and Papua New Guinea. Aust. J. Exp. Biol. Med. Sci. 64 (6), 571–585.

Lobigs, M., Marshall, I.D., Weir, R.C., Dalgarno, L., 1988. Murray Valley encephalitis virus field strains from Australia and Papua New Guinea: studies on the sequence of the major envelope protein gene and virulence for mice. Virology 165, 245–255.

Lobigs, M., Mullbacher, A., Wang, Y., Pavy, M., Lee, E., 2003. Role of type I and type II interferon responses in recovery from infection with an encephalitic flavivirus. J. Gen. Virol. 84, 567–572.

Mason, P.W., Shustov, A.V., Frolov, I., 2006. Production and characterization of vaccines based on flaviviruses defective in replication. Virology 351, 432–443.

Müller, U., Steinhoff, U., Reis, L.F., Hemmi, S., Pavlovic, J., Zinkernagel, R.M., Aguet, M., 1994. Functional role of type I and type II interferons in antiviral defence. Science 264, 1918–1921.

Orlinger, K.K., Hoenninger, V.M., Kofler, R.M., Mandl, C.W., 2006. Construction and mutagenesis of an artificial bicistronic tick-borne encephalitis virus genome reveals an essential function of the second transmembrane region of protein e in flavivirus assembly. J. Virol. 80 (24), 12197–12208.

Patkar, C.G., Kuhn, R.J., 2008. Yellow fever virus NS3 plays an essential role in virus assembly independent of its known enzymatic functions. J. Virol. 82, 3342–3352.

Pijlman, G.P., Kondratieva, N., Khromykh, A.A., 2006. Translation of the flavivirus kunjin NS3 gene in *cis* but not its RNA sequence or secondary structure is essential for efficient RNA packaging. J. Virol. 80, 11255–11264.

Samuel, M.A., Diamond, M.S., 2005. alpha/beta Interferon protects against lethal West Nile virus infection by restricting cellular tropism and enhancing neuronal survival. J. Virol. 79, 13350–13361.

Scholle, F., Girard, Y.A., Zhao, Q., Higgs, S., Mason, P.W., 2004. *trans*-Packaged West Nile virus-like particles: infectious properties in vitro and in infected mosquito vectors. J. Virol. 78, 11605–11614.

Schrauf, S., Mandl, C.W., Bell-Sakyi, L., Skern, T., 2009. Extension of flavivirus protein C differentially affects early RNA synthesis and growth in mammalian and arthropod host cells. J. Virol. 83, 11201–11210.

Smith, T.J., Brandt, W.E., Swanson, J.L., McCown, J.M., Buescher, E.L., 1970. Physical and biological properties of dengue-2 virus and associated antigens. J. Virol. 5, 524–532.

Stocks, C.E., Lobigs, M., 1995. Posttranslational signal peptidase cleavage of the flavivirus C–prM junction, in vitro. J. Virol. 69, 8123–8126.

Stocks, C.E., Lobigs, M., 1998. Signal peptidase cleavage at the flavivirus C–prM junction: dependence on the viral NS2B-3 protease for efficient processing requires determinants in C, the signal peptide, and prM. J. Virol. 72, 2141–2149.

Stollar, V., 1969. Studies on the nature of dengue viruses: IV. The structural proteins of type 2 dengue virus. Virology 39, 426–438.

Varnavski, A.N., Young, P.R., Khromykh, A.A., 2000. Stable high-level expression of heterologous genes in vitro and in vivo by noncytopathic DNA-based Kunjin virus replicon vectors. J. Virol. 74, 4394–4403.

von Heijne, G., 1990. The signal peptide. J. Membr. Biol. 115, 195–201.

Yamshchikov, V.F., Compans, R.W., 1993. Regulation of the late events in flavivirus protein processing and maturation. Virology 192, 38–51.

Zhang, Y., Corver, J., Chipman, P.R., Zhang, W., Pletnev, S.V., Sedlak, D., Baker, T.S., Strauss, J.H., Kuhn, R.J., Rossmann, M.G., 2003. Structures of immature flavivirus particles. EMBO J. 22, 2604–2613.